Journal of Solid State Chemistry **145,** 336–344 (1999)
Article ID jssc.1999.8293, available online at http://www.idealibrary.com on IDEAL®

Intercalation and Deintercalation Processes for Ammoniated 1T-TaS_2

Lisa Diebolt,* William Glaunsinger,*,†,[1] and Michael McKelvy†

*Department of Chemistry and Biochemistry and †Center for Solid State Science, Arizona State University, Tempe, Arizona 85287-1704

Received July 10, 1998; in revised form March 18, 1999; accepted March 23, 1999

The intercalation and deintercalation processes for nearly stoichiometric 1T-TaS_2 have been investigated by X-ray powder diffraction, thermogravimetric analysis, differential scanning calorimetry, and mass spectrometry. The maximum ammonia stoichiometry that has been prepared for a 4-month reaction time is $(NH_4^+)_{0.06}$ $(NH_3)_{0.07}$ $(1T\text{-}TaS_2)^{0.06-}$. The reaction mechanism can be accounted for within a redox-rearrangement model in which part of the NH_3 is oxidized to NH_4^+ upon intercalation, with the NH_4^+ decomposing at the host-layer edges to liberate NH_3 and H_2 upon deintercalation. All intercalation compounds prepared could be deintercalated at relatively low temperatures. The intercalates retained some 1T-TaS_2 host material, which may be associated with the rather low concentration of intercalant combined with intercalation reaction fronts that only partially penetrate the host in a nucleation and growth process. This study indicates that ammoniated 1T-TaS_2 is a unique redox-rearrangement intercalation system. © 1999 Academic Press

INTRODUCTION

Group V transition metal dichalcogenides (TMDs) may adopt either octahedral or trigonal prismatic coordination of their host layers, or a combination of both, resulting in the existence of various polytypes of the same TMD. Jellinek investigated the structural polytypes of TaS_2 and found that several types can be prepared using different reaction conditions and annealing temperatures (1). Among TaS_2 polytypes, 1T-TaS_2 has attracted special interest because of the wide range of structural and electronic properties that this material and its intercalates exhibit.

Interest in this system started when electrical resistivity measurements showed that 1T-TaS_2 undergoes two first-order phase transitions, one at ~ 350 K and the other centered at ~ 200 K, with large hysteresis (2). However, it was not until 1974 that detailed electron diffraction studies showed that these anomalies were associated with charge-density-wave (CDW) distortions (3, 4). Fermi-surface instabilities lead to the formation of CDWs, which are coupled periodic distortions of the conduction electron density and the underlying atomic lattice that produce superlattice structures. Strong CDW distortions have been found for 1T-TaS_2, where the superlattice is incommensurate from 353 to 543 K, nearly commensurate between 200 and 353 K, and commensurate below 200 K (5). Recently, scanning tunneling microscopy has been used to provide atomic-level images of these intriguing superlattices (6–8).

Many studies of 1T-TaS_2 intercalation chemistry have involved investigations of molecular guests. In particular, there have been several investigations of hydrazine intercalation of 1T-TaS_2 (9, 10). This system is of interest because it provides a rare example of a molecular intercalation process that results in substantial guest–host charge transfer (11). Experimental evidence suggests that the gaseous intercalation process involves direct electron transfer, with orbital mixing of the hydrazine lone pairs with available host-layer states. This finding is consistent with the tendency for charge transfer to be the driving force for intercalation reactions (10, 12). In this case, the degree of charge transfer and the resulting chemical nature of the guest are of fundamental importance in understanding the relationship between charge transfer and intercalation. Essentially complete charge transfer occurs when alkali metals are inserted into transition-metal disulfide (TS_2) lamellar materials (12, 13), but for molecular intercalates the role of charge transfer and the nature of the guest–host interactions are still largely unresolved. Although larger amines such as pyridine (14) and long-chain amines (15) also intercalate, the thermal irreversibility of these reactions makes it difficult to follow the chemistry of their intercalation/deintercalation processes. Therefore, this study focuses on the simple prototypical Lewis base NH_3.

Several different structural models have been proposed to describe the arrangement of ammonia species within the TS_2 matrix (16–21). The optimum orientation for direct orbital overlap and guest–host charge transfer occurs if the ammonia lone pair is directed perpendicular to the TS_2 host layers, as shown in Fig. 1a. However, a single-crystal proton NMR study revealed that the C_3 axis of the intercalated ammonia molecule is parallel, rather than perpendicular, to

[1] To whom correspondence should be addressed.

0022-4596/99 $30.00

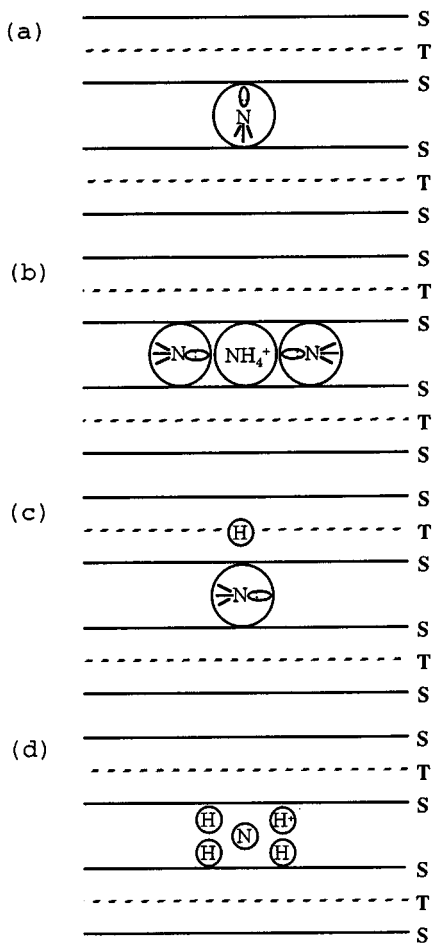

FIG. 1. Four possible arrangements for ammonia species in layered TS_2 compounds. The orientation with optimum host-layer orbital overlap is shown in (a). The redox-rearrangement model, in which ammonia molecules are cointercalated with ammonium ions, is depicted in (b). The hydride model in (c) considers H as a cointercalated species that is located at intralayer sites. In (d), intercalated H, N, and H^+ exist as separate entities in the "dissociated-ammonia" model. In (b) and (d), one electron per cation is transferred to the TS_2 layers to achieve electronic neutrality.

the host layers in 2H-TaS_2 (22). An explanation for the parallel orientation was first proposed by Schöllhorn and Zagefka during an investigation of ammonia intercalation of 2H-TaS_2 (18). They proposed that redox reactions involving the formation of new products are often involved in the molecular intercalation of TS_2 compounds. In particular, the ammonia intercalation of 2H-TaS_2 was described by a redox reaction in which NH_4^+ ions are formed and cointercalated with NH_3, as depicted in Fig. 1b, which favors a parallel orientation of NH_3 to maximize ion–dipole interactions. The proposed reaction mechanism (18) can be described by the reactions:

$$\frac{y'}{3}\,NH_3 \rightarrow \frac{y'}{6}\,N_2 + y'H^+ + y'e^-, \qquad [1]$$

$$y'H^+ + y'NH_3 \rightarrow y'NH_4^+, \qquad [2]$$

$$y'e^- + TS_2 \rightarrow TS_2^{y'-}. \qquad [3]$$

This redox-rearrangement mechanism has also been suggested for the NH_3 intercalation of TiS_2 and NbS_2 (16, 17).

In an alternative model, it has been proposed that hydride formation occurs during ammonia intercalation into 2H-TaS_2 (20), with the excess protons occupying intralayer positions, as shown in Fig. 1c. Neutron powder diffraction data on D_xTaS_2 and $H_{0.76}NbS_2$ have provided structural evidence that intercalated hydrogen can reside within the host layers, where each H is located at the center of an equilateral triangle formed by three tantalum or niobium atoms, respectively (22).

The "dissociated-ammonia" model provides yet a different interpretation of the redox process (21). Here it is assumed that the intercalation process results in decoupling of the nitrogen and hydrogen atoms in the individual ammonia molecules, accompanied by intercalation of protons in response to the electron acceptor behavior of the host. The dissociated nitrogen atoms are proposed to occupy trigonal prismatic sites surrounded by rapidly exchanging hydrogen atoms and protons in neighboring sites. A schematic diagram illustrating the presence of decoupled N and H atoms as well as H^+ is shown in Fig. 1d.

There is substantial evidence that the intercalation of NH_3 into 2H-TaS_2, TiS_2, and NbS_2 involves redox rearrangement. For all three compounds, N_2 is evolved during the intercalation process, as described by reaction [1] of the redox-rearrangement model (16–18). Also, SQUID measurements of the metallic paramagnetism of these materials indicate that guest–host charge transfer is achieved by the transfer of 1 mole e^-/mole NH_4^+ to the host conduction band, with no charge transfer being associated with intercalated NH_3 (16, 17). X-ray photoelectron spectroscopy (XPS) experiments on metal–ammonia intercalates also demonstrates that NH_3 and NH_4^+ coexist within the vdW gap (23). Therefore, these intercalation compounds are best described by the formula $(NH_4^+)_{y'}(NH_3)_{y''}TS_2^{y'-}$, where $y' = 0.23 \pm 0.02$ for TiS_2 and NbS_2 (16, 17). For 2H-TaS_2, $y' \approx 0.10$ was estimated from ion exchange of NH_4^+ with KBr in liquid NH_3 (18). Thus, the extent of charge transfer during ammonia intercalation is substantially lower for 2H-TaS_2 than for TiS_2 and NbS_2.

Ideally, intercalation reactions are reversible, so that deintercalation should regenerate the original host matrix and guest species. Deintercalation of NH_3 and NH_4^+ from TiS_2 and NbS_2 occurs at relatively low temperatures, with essentially complete regeneration of the host structures, illustrating the reversibility of intercalation for these systems. The deintercalation process for these reactions

consists of two steps:

$$(NH_4^+)_{y'}(NH_3)_{y''}TS_2^{y'-} \rightarrow y''NH_3 + (NH_4^+)_{y'}TS_2^{y'-}, \quad [4]$$

$$(NH_4^+)_{y'}TS_2^{y'-} \rightarrow \frac{y'}{2}H_2 + y'NH_3 + TS_2. \quad [5]$$

However, the deintercalated material is not entirely identical to the original host, as the layers do not shift back into perfect host-layer registry (17, 24).

Previous studies have demonstrated that 1T-TaS_2 does not form intercalation compounds as readily as 2H-TaS_2 (25). In fact, monophasic stage-1 ammoniated 1T-TaS_2 has not yet been prepared. Bouwmeester *et al.* were able to obtain crystallographic data from ammoniated 1T-TaS_2 prepared in an autoclave (the ammonia content of this material was not provided and a mixture of phases was present) (26). However, the nature of the guest species and the mechanism of charge transfer have not been elucidated for this system, which are the goals of this study. In order to accomplish these goals, it is important to minimize side reactions by using pure starting materials, rigorously excluding water, and carrying out the reactions at low temperatures.

This study has employed several complementary techniques, including X-ray powder diffraction (XPD), mass spectrometry, vapor-pressure measurements (VPM), thermogravimetric analysis (TGA), and differential scanning calorimetry (DSC), to elucidate the nature of the guest species as well as the intercalation/deintercalation mechanisms for the ammonia intercalation of 1T-TaS_2. The results of this work are compared to those obtained for ammoniated 2H-TaS_2, TiS_2, and NbS_2 in order to obtain a more comprehensive view of ammonia intercalation in TS_2 hosts. These intercalation systems are of particular interest because of their uniquely high level of thermal reversibility and the simplicity of their reactant and intercalant species. They provide good model systems to further the understanding of more complex Lewis base/TS_2 intercalation systems, which are usually more difficult to characterize.

EXPERIMENTAL

1. Host

Polycrystalline TaS_2 samples were synthesized by directly reacting sulfur (Aldrich Chemical Company, 99.999%, or Alfa Products, 99.9995%) and tantalum wire (0.02″ diam., Material Research Corp., 99.95%). Wire portions of Ta weighing approximately 1 g were sized using wire cutters with plastic-covered tips and tied into bundles. The wire bundles were then placed in a beaker containing reagent grade trichloroethylene (J. T. Baker, $< 0.0001\%$ evaporation residue) and sonicated for 15 min. A second trichloroethylene sonication was followed by three sonications in reagent grade toluene (J. T. Baker, $< 0.00001\%$ evaporation residue) to ensure that all grease from wire processing and handling was removed from the surface of the wire.

Stoichiometric amounts of Ta and S, plus an additional 1 mg/cm^3 excess sulfur, were added to quartz ampoules. The addition of the excess sulfur helps stabilize the formation of the 1T polytype (27). The quartz ampoules were then evacuated to 10^{-4} Torr and flame-sealed. The samples were placed in a furnace and heated to 450°C. The temperature was maintained at 450°C for 2 days, then raised 50°C/day to a final temperature of 950°C. After 7 days at 950°C, the samples were removed and vigorously shaken to expose unreacted wire. The ampoules were transferred to the furnace and held at 950°C for an additional 10 days. The 1T polytype is obtained by removing the samples from the furnace at 950°C and rapidly quenching the ampoules in a container of water. If unreacted wire was observed, the samples were heated at 950°C for an additional 2–3 days, and this procedure was repeated until unreacted wire was not visible. Excess sulfur was sublimed away from the resulting golden-metallic 1T-TaS_2 material to the opposite end of the ampoule.

The ampoules were transferred into a helium-filled glove box (< 1 ppm H_2O and O_2) and opened. The product was poured into an agate mortar and gently crushed. All host samples in this study were stored in weighing bottles in the glovebox and only removed from the glove box in leak-checked, sealed containers to prevent surface hydrolysis/oxidation in air. The resulting stoichiometry of the 1T-TaS_2 was determined by oxidation to Ta_2O_5 in pure oxygen using a Perkin–Elmer TGS-2 TGA system having 0.1 mg sensitivity and 0.01% weight resolution.

XPD patterns were recorded at ambient temperature using photographic film as well as a Rigaku diffractometer standardized with NBS standard 640 silicon. All patterns were obtained using Ni-filtered Cu$K\alpha$ radiation.

2. Intercalate

Ammoniated 1T-TaS_2 compounds were prepared by reaction of liquid NH_3 (99.9% purity from Matheson Gas Products; dried over sodium) with 1T-TaS_2 in a sealed pyrex n-cell (16, 17). At the beginning of the reaction process, the n-cell was sonicated in distilled water for 5 min. Sonication creates smaller particles that intercalate more readily, but care must be exercised as the reaction vessel contains 10 atm pressure NH_3. To further accelerate intercalation, the 1T-TaS_2 samples were first intercalated with NH_3, thermally deintercalated at 250°C to help loosen the host layers, and subsequently reintercalated. Even with this procedure, ammonia intercalation of 1T-TaS_2 is a kinetically slow process, so samples were equilibrated in liquid NH_3 for 1–12 months.

To obtain the pure intercalate, traces of polysulfides created during intercalation were removed from the residual NH_3 in the sample leg of the n-cell by repeated decanting of liquid NH_3 from the sample-containing leg to the opposite leg followed by vacuum distilling the ammonia back onto the intercalate using an ice-water bath (24). It is important to store the intercalate in sealed ampoules, since the intercalate continuously loses NH_3 when left in a weighing bottle in the glove box (16, 17). Since intercalated TaS_2 is extremely sensitive to air and moisture, it was only removed from the glove box in leak-checked, sealed containers.

Evolved-gas analysis was performed during thermal deintercalation of ammoniated TaS_2 using a quadrupole mass spectrometer (Hiden Analytical Laboratories model HAL-201) and a Baratron manometer connected to a vacuum line. Typically, deintercalation was achieved by slowly heating (1–3°C/min) the sample to 250°C. After deintercalation was complete, the intercalate was isolated, and the condensable, deintercalated gas was condensed in a gas bulb at -196°C. Mass spectral analysis of the noncondensable gas was accomplished by expanding the gas remaining in the vacuum line into the mass spectrometer. After the noncondensable gas was removed, the condensable gas was analyzed by warming the gas bulb to ambient temperature.

Intercalate stoichiometry was determined by both VPM and TGA. Vapor-pressure measurements of the total gas evolved were recorded at temperature intervals of 20°C. To obtain accurate pressure measurements for the noncondensable gas, the intercalate was first isolated from the evolved gas in the vacuum line. Then the condensable evolved gas was condensed in a liquid-nitrogen cold trap. Once the pressure stabilized and remained constant for at least 20 min, a pressure–volume–temperature (PVT) data point was recorded. The partial pressure of the condensable gas was determined as the difference between the total pressure and the noncondensable gas pressure. Since ammoniated TaS_2 is very sensitive to air and moisture, TGA samples for deintercalation analysis were loaded in aluminum pans and hermetically sealed in the glove box. The pans were loaded into sealed Ball jars and transferred to the TGA system, which was housed in a nitrogen-containing glove box. A small pinhole was punched in the top of the pans just prior to their insertion into the TGA. Purified Ar was used as the TGA carrier gas (24).

Elemental analysis was performed on both the original and deintercalated hosts by Galbraith Laboratories to quantify any nitrogen remaining in the sample after thermal deintercalation.

Calorimetry measurements were performed using a Perkin–Elmer DSC-4 differential scanning calorimeter. The melting transition of indium was used to calibrate both the temperature and enthalpies observed. Nitrogen carrier gas was slowly passed through a cold trap at -78°C to reduce any residual water to <1 ppm. The samples were loaded into aluminum pans, sealed hermetically, and handled in the same manner as the TGA samples. The loading chamber of the instrument was enclosed by a homemade glove bag flushed with nitrogen to allow inert sample transfer into the analysis chamber. The heating rate and sample weight were optimized, with typical values being 5°C/min and 10–15 mg of sample, respectively. Intercalate XPD patterns were recorded using photographic film and a Debye–Scherrer camera, which was previously calibrated with NBS-standard 640 silicon. The samples were loaded in 0.3 mm pyrex capillaries in the glove box under an atmosphere of helium. The capillaries were isolated with a stopcock assembly and removed from the box. The capillaries were then flame-sealed for XPD analysis. Selected capillaries were rerun several weeks later to check that the X-ray powder pattern did not change with time. All patterns were obtained using Ni-filtered Cu$K\alpha$ radiation.

RESULTS AND DISCUSSION

1. *Characterization*

The 1T-TaS_2 prepared for this study had sharp XPD reflections that could be indexed to a hexagonal cell having lattice parameters of $a = 3.365(1)$ Å and $c = 5.853(1)$ Å. These parameters are in good agreement with those of Hägg and Schönberg (28).

A typical TGA curve of the oxidation of 1T-TaS_2 is shown in Fig. 2. The small increase in the weight percentage prior to the weight-loss region is most likely due to sulfate formation (29). The resulting stoichiometry of the host was $Ta_{1.002 \pm 0.001}S_2$. This nearly stoichiometric host is well suited for intercalation studies, since the excess metal that can pin the host layers together and impede intercalation is minimal (11).

Since ammonia deintercalation commences immediately upon exposing the intercalate to ambient glove box

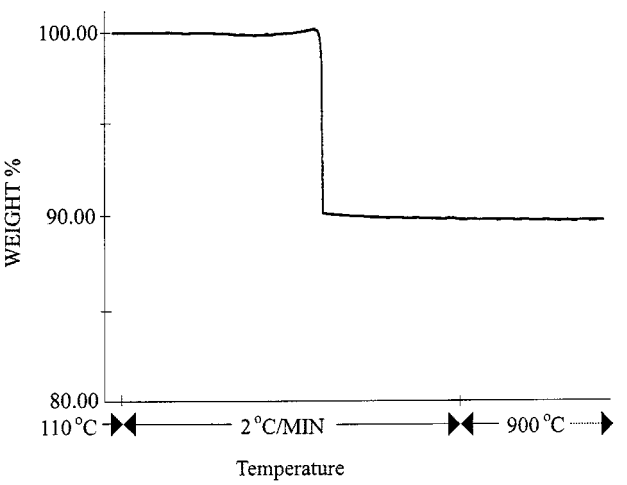

FIG. 2. A typical TGA curve of the oxidation of TaS_2 to Ta_2O_5 in oxygen.

conditions (16, 17), samples for XPD investigations using photographic film were also prepared by equilibrating the intercalate with 500 Torr of pure NH_3. Ammoniated 1T-TaS_2 samples prepared by this "back-filling" method contained approximately 0.26 moles of NH_3 per mole of 1T-TaS_2, as determined by PVT measurements of the deintercalation of samples of the intercalate initially under 500 Torr of NH_3.

As a result of the low concentration of guest species, the X-ray patterns of ammoniated 1T-TaS_2 samples were always found to contain several reflections indexable to the host structure. The only peak (intermediate intensity) that could not be indexed to the host material was observed at 9.12 Å. This reflection is in good agreement with the 003 reflection observed for the structure of 3R-TaS_2NH_3 (9.117 Å) prepared from 1T-TaS_2 (26). In the 3R structure, the 1T-TaS_2 layers shift with respect to each other, but there is no change in structure within the host layers. However, the 003 reflection is only observed after back-filling the sample with 500 Torr of NH_3. It appears that partial intercalation coupled with the associated elastic stress enhances deintercalation under ambient glove box conditions. Since only one reflection distinct from those of the host was observable, unit-cell parameters of the intercalate cannot be assigned or compared to those obtained previously under less rigorously anhydrous synthetic conditions (26).

Upon thermal deintercalation of the intercalate, the original 1T-TaS_2 pattern is obtained. The cell parameters for a typical deintercalated 1T-TaS_2 sample are $a = 3.365(2)$ Å and $c = 5.86(2)$ Å.

2. Deintercalation Process

The identity of the gaseous species evolved during thermal deintercalation was determined by mass spectrometry. As expected, the peaks observed for the condensable gas (amu 17, relative intensity 100; amu 16, relative intensity 95; amu 15, relative intensity 12; amu 14, relative intensity 3) are characteristic of the fragmentation pattern of NH_3 (30). The mass spectrum of the noncondensable fraction confirms that the noncondensable gas is essentially pure H_2 (amu 2, relative intensity 100; amu 1, relative intensity 41). No other peaks were found in either spectrum, except those due to trace amounts of N_2, O_2, and H_2O, which were also present in the background spectra. Importantly, no peaks attributable to H_2S (33 and 34 amu) were observed in the spectra obtained during thermal deintercalation of ammoniated 1T-TaS_2. The absence of H_2S indicates that the host layers have not been attacked by moisture and such host degradation has not occurred (31).

Figure 3 shows the identity and pressure of volatile species deintercalated as a function of temperature for an ammoniated 1T-TaS_2 sample, as determined by mass spectrometry and vapor-pressure measurements. It is evident

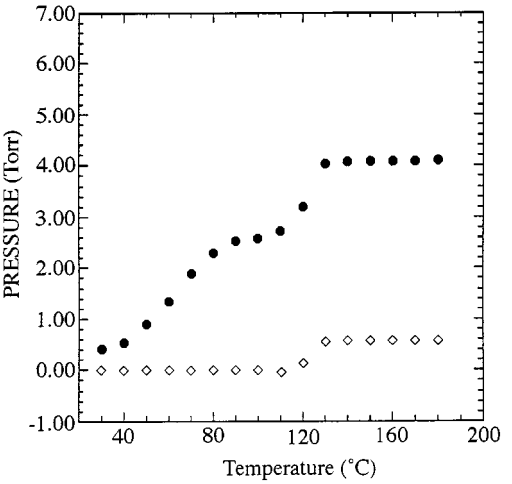

FIG. 3. The pressure of NH_3 (●) and H_2 (◇) deintercalated versus temperature, as determined by mass spectrometry and vapor pressure measurements. The sample used in this experiment was $(NH_4^+)_{0.05}(NH_3)_{0.07}$ $(1T\text{-}TaS_2)^{0.05-}$.

that two separate thermal events occur during deintercalation. The first event ($< 100°C$) corresponds to the evolution of the more loosely bound NH_3. H_2 evolution is observed concurrently with NH_3 deintercalation during the second event (between 100 and 140°C), which suggests a correlation between H_2 and more strongly held ammonia. The simultaneous deintercalation of NH_3 and H_2 during the second event can be attributed to NH_4^+ deintercalation. The total ratio of NH_3 to H_2 evolved during the second step was 0.72 to 0.28 ± 0.01. This ratio is slightly greater than the 2:1 ratio of $NH_3:H_2$ observed during deintercalation of ammonium from ammoniated 1T-TiS_2 (16, 24). This difference arises from a small degree of overlap between the ammonia and ammonium deintercalation steps, since all of the weakly bound NH_3 has not completely deintercalated before NH_4^+ begins to deintercalate. This results in low H_2 percentages during the initial deintercalation of ammonium. A small amount of overlap between the first and second steps was also found during the thermal deintercalation of ammoniated NbS_2 (17, 32), where the ratio of NH_3 to H_2 evolved during the second step was 0.70 to 0.30. From the amounts of gases evolved and Eqs. [4] and [5], the composition of the typical intercalate shown in Fig. 3 is $(NH_4^+)_{0.05}$ $(NH_3)_{0.07}(1T\text{-}TaS_2)^{0.05-}$.

A typical TGA of ammoniated 1T-TaS_2, which was reacted with ammonia for approximately four months, is shown in Fig. 4. From the overall weight loss, the nominal content of ammonia is 0.13 mole NH_3/mole 1T-TaS_2. Two well-defined steps are evident for the deintercalation process, corresponding to the deintercalation of ammonia ($< 100°C$) and ammonium (100–150°C). This two-step deintercalation process is consistent with results found during the deintercalation of ammoniated TiS_2 and NbS_2 (16, 17). Similarly, the composition of this intercalate is determined from the

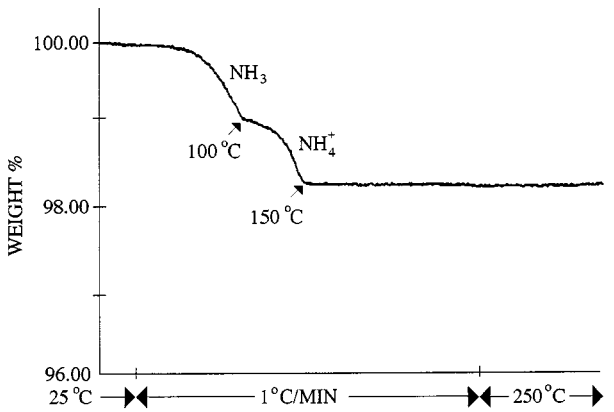

FIG. 4. A typical TGA curve for ammoniated 1T-TaS_2. Two distinct weight losses are observed due to volatile species evolved from the intercalate: (1) weakly bound ammonia and (2) more strongly bound ammonium ions.

TGA curve to be $(NH_4^+)_{0.06}(NH_3)_{0.07}(1T\text{-}TaS_2)^{0.06-}$, which is within experimental error of that determined by vapor-pressure measurements. Compositions determined by TGA and VPM typically agreed within $\pm$ 0.01.

The ammonia intercalation of 1T-TaS_2 proceeds much more slowly than the ammonia intercalation of TiS_2, NbS_2, or 2H-TaS_2. Table 1 shows that the intercalant composition increases with exposure time to NH_3. Complete intercalation was not observed, even for samples that were reacted with NH_3 for several months. This behavior is in contrast to the essentially complete ammonia intercalation of 2H-TaS_2 in several hours (33). Sonication and repetitive intercalation/deintercalation of NH_3 increased the amount of NH_3 intercalated, but still did not lead to substantial intercalation. Intercalation at temperatures above ambient was not attempted due to the risk of host-lattice attack (trace amounts of polysulfide are already observed for ambient-temperature intercalation) that could invalidate comparisons of the intercalation and deintercalation chemistry of 1T-TaS_2 with that of the aforementioned hosts.

Elemental analysis of deintercalated 1T-TaS_2 showed that there is no residual nitrogen within the accuracy of the measurement (< 0.005 mole N/mole TaS_2), which confirms complete NH_3/NH_4^+ deintercalation.

TABLE 1
Reaction Time for Different Intercalate Stoichiometries in $(NH_4^+)_{y'}(NH_3)_{y''}(1T\text{-}TaS_2^{y'-})$

Analytical method	y'	y''	Reaction time (days)
TGA	0.02	0.02	14
TGA	0.02	0.05	65
TGA	0.05	0.06	95
TGA	0.06	0.07	130
VPM	0.02	0.06	65
VPM	0.05	0.07	130

3. Energetics

DSC revealed that three distinct thermal events are observed during the thermal deintercalation of $(NH_4^+)_{0.06}(NH_3)_{0.07}(1T\text{-}TaS_2)^{0.06-}$, as shown in Fig. 5. The sharp peak at 80°C is attributed to a transition from a nearly commensurate superlattice to an incommensurate superlattice in the residual host material. Such a first-order phase transition at about 353 K was observed during DSC investigations of 1T-TaS_2 (5). The onset temperatures of the other two endothermic peaks are in good agreement with those determined from TGA experiments. Thus, the peak at $\sim$100°C is assigned to ammonia deintercalation, whereas the peak at $\sim$150°C is due to ammonium deintercalation. The enthalpies for ammonia and ammonium deintercalation are 6.0 kcal/mole NH_3 and 20 kcal/mole NH_4^+, respectively. These values were reproducible to $\pm$ 20%.

The ammonia and ammonium deintercalation enthalpies for ammoniated 1T-TaS_2 are consistent with those obtained for ammoniated TiS_2 (34), NbS_2 (17), and 2H-TaS_2 (33). The deintercalation enthalpies for these four ammoniated hosts are summarized in Table 2. The substantially higher enthalpies associated with ammonium deintercalation indicate that this species is more strongly bound between the host layers than ammonia, due to the stronger ionic forces between NH_4^+ and the negatively charged TS_2 layers. The similar deintercalation enthalpies observed for the different hosts suggests similar guest–host and guest–guest interactions for NH_3 and NH_4^+ in these intercalates. The somewhat

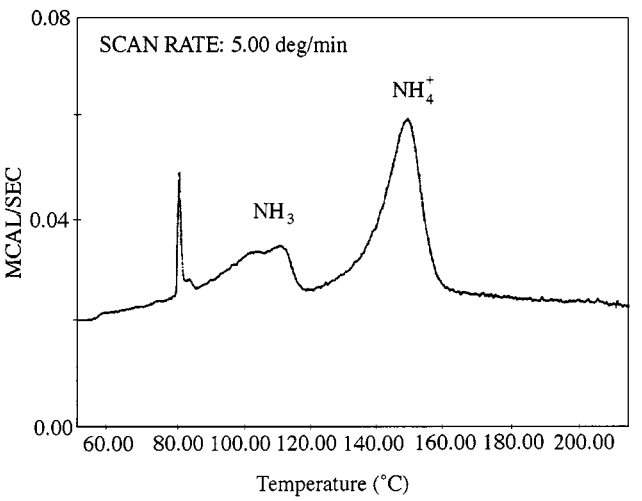

FIG. 5. A typical DSC curve for ammoniated 1T-TaS_2. The two endothermic transitions that are observed at higher temperatures are due to NH_3 and NH_4^+ deintercalation. The sharp peak observed at approximately 80°C is associated with the presence of some unintercalated 1T-TaS_2 host material, as discussed in the next.

TABLE 2
Deintercalation Enthalpies for NH_3 and NH_4^+ in Ammoniated TS_2 Compounds

Compound	ΔH_{NH_3} (kcal/mole)[a]	$\Delta H_{NH_4^+}$ (kcal/mole)[a]
$(NH_4^+)_{0.06}(NH_3)_{0.07}(1T\text{-}TaS_2^{0.06-})$	6.0	20
$(NH_4^+)_{0.22}(NH_3)_{0.23}TiS_2^{0.22-}$	10.5[b]	22[b]
$(NH_4^+)_{0.23}(NH_3)_{0.48}NbS_2^{0.23-}$	7.6[c]	18.5[c]
$(NH_4^+)_{0.08}(NH_3)_{0.84}(2H\text{-}TaS_2^{0.08-})$	8[d]	19[d]

[a] Values are precise to $\pm 20\%$.
[b] From Ref. (34).
[c] From Ref. (17).
[d] From Refs. (33) and (34).

lower value for ΔH_{NH_3} for the 1T-TaS_2 intercalate may be associated with incomplete intercalation and the release of elastic strain associated with guest islands, guest edge dislocations, etc., during deintercalation (35). Unlike the ammonia 1T-TaS_2 intercalate, the other three intercalations are initially stage 1, without the residual elastic strain associated with partial intercalation.

It is interesting to consider the possibility of different energetic sites for the intercalated ammonia species. Indeed, the character of the NH_3 DSC peak suggests this possibility. However, the relatively well-defined deintercalation steps observed by TGA and DSC for NH_3 and NH_4^+ compared to the small overlap between these steps observed in the vapor-pressure measurements are not likely associated with such differences. Rather, they are probably associated with the low vapor pressure of NH_3 over the TGA and DSC samples, where NH_3 is constantly swept away by the inert flow gas, relative to the much higher vapor pressure of NH_3 over the vapor-pressure sample near the step transition ($\sim$2–4 Torr). Such a vapor pressure of NH_3 over the sample will increase the temperature at which it is evolved for a given intercalate NH_3 content.

4. Reaction Mechanisms

The redox-rearrangement model provides a good overall description of the ammonia intercalation process for TiS_2 and NbS_2 as well as for both 2H-TaS_2 and 1T-TaS_2. VPM, TGA, and DSC results suggest that the mechanism of deintercalation for ammoniated 1T-TaS_2 follows the reactions observed for the ammoniated 2H-NbS_2 and 1T-TaS_2 systems, with no retention of nitrogen in the deintercalated host. Hence, the intercalation of NH_3 into 1T-TaS_2 appears to be a reversible redox-rearrangement process. Since NH_4^+ "deintercalation" occurs with simultaneous NH_3 and H_2 evolution in an approximate 2 : 1 ratio according to Eq. [5], NH_4^+ decomposition upon deintercalation probably does not occur within the 1T-TaS_2 host. Instead, the experimental evidence is consistent with NH_4^+ diffusing to the edge of the host layers, where it decomposes to liberate stoichiometric amounts of NH_3 and H_2 (24).

Experimental evidence from previous investigations indicates that NH_3 intercalates much more readily into TiS_2, NbS_2, and 2H-TaS_2 than it does into 1T-TaS_2. Several factors may contribute to the difficulty of intercalating 1T-TaS_2, including differences in the electronic-structure-driven interactions during intercalation, the structural arrangement of atoms (including defect type and density), the presence of nonstoichiometric host material, and the synthesis conditions.

The XPD patterns of 1T-TaS_2 have sharp diffraction lines, indicating that the 1T-TaS_2 host lattice is highly ordered (1, 36). This is in contrast to the patterns obtained for 2H-TaS_2, where the $h - k \neq 3n$ lines are broadened (1), indicating the presence of stacking disorder. Such disorder probably occurs during the synthesis of 2H-TaS_2, which involves slow cooling the reaction product from 950°C (1, 37). In this process, the initially formed 1T-TaS_2 is transformed at lower temperatures to 2H-TaS_2. This transition causes considerable structural disorder in the stacking of 2H-TaS_2 layers. Such disorder has been associated with internal-gallery intercalation onset, which has the potential to enhance intercalation reactivity (38). Microcracks associated with the 1T-2H transition have also been observed on the surface of 2H-TaS_2 crystals (37). These microcracks provide substantial additional edge area and edge defects that can also enhance intercalation and, hence, contribute to the higher reactivity of 2H-TaS_2 relative to 1T-TaS_2 (38).

A neutron diffraction investigation of the intercalation of the related materials $K_{0.3}{}^+(H_2O)_{0.7}[1T\text{-}TaS_2]^{0.3-}$ and $K_{0.5}{}^+(H_2O)_{0.5}[2H\text{-}TaS_2]^{0.5-}$ indicated that different reaction pathways occur for the two different polytypes. Whereas higher-stage intermediates are routinely formed during 2H-TaS_2 intercalation, only transient high-stage intermediate nuclei are formed with the 1T polytype at the onset of intercalation (39). These quickly convert to a two-phase region, 1T-TaS_2/$K_{0.3}^+(H_2O)_{0.7}[1T\text{-}TaS_2]^{0.3-}$, which persists during the cathodic reduction of 1T-TaS_2. The reduction of 1T-TaS_2 in a K^+/H_2O electrolyte results in the final product, $K_{0.3}^+(H_2O)_{0.7}[1T\text{-}TaS_2]^{0.3-}$, with a lower negative-layer charge density than observed for $K_{0.5}^+(H_2O)_{0.5}[2H\text{-}TaS_2]^{0.5-}$, which is formed under the same reaction conditions (39). The lower charge transfer observed for the former product inhibits ordered-stage formation, which is typically driven by electrostatic repulsion between the charged layers.

This same phenomenon may also occur during the ammonia intercalation of 1T-TaS_2, where a two-phase, stage 1 intercalate/host material is obtained as the reaction product. At the atomic level, intercalation processes can begin in outermost galleries, where less elastic strain is associated with deforming the host layers and adsorbate–host charge transfer can assist intercalation, or at internal galleries

associated with defects (38). Subsequent intercalation progression primarily proceeds layer by layer away from the outermost and internal onset galleries (35, 38, 40–43). In this regard, highly ordered 1T-TaS_2 crystallites may structurally contribute to their slow intercalation kinetics via a paucity of surface and/or internal structural defects that can promote internal intercalation onset (38). This would limit the reaction process to preferential intercalation of the outermost galleries, potentially accumulating host-layer elastic strain that can further inhibit intercalation (42).

Previous investigations of ammoniated TiS_2 and NbS_2 indicated that NH_4^+ deintercalates above 150°C. In comparison, NH_4^+ deintercalation is essentially complete at 150°C for 1T-TaS_2. The lower temperatures observed for NH_3 and NH_4^+ deintercalation from the 1T-TaS_2 intercalate may be due to the relatively small concentration of guest species present in this intercalate and residual host-layer elastic strain present in these partially intercalated materials. Theoretical studies of graphite intercalation compounds containing a low concentration of intercalate ions have found that the graphite layers are significantly strained due to partial gallery occupation (42). Such elastically strained host layers in ammoniated 1T-TaS_2 may facilitate deintercalation to minimize their elastic strain energy. Furthermore, should the outermost galleries be preferentially intercalated, their deintercalation should occur at lower temperatures. This follows from their lower deintercalation activation energy due to the greater flexibility of their neighboring host layers (35, 44).

CONCLUSION

The results of this study indicate that there are two chemically distinct types of ammonia in ammoniated 1T-TaS_2: NH_3 and NH_4^+. Both intercalation and deintercalation processes can be understood within a redox-rearrangement framework. Such redox-rearrangement reactions can strongly influence both the chemical and physical properties of the resulting intercalation complexes. The unique features of this system are the relatively low concentration of intercalant, the low deintercalation temperatures of NH_3 and NH_4^+, and the potential intergrowth of the host and intercalate during intercalation via primarily outside-in intercalation of the host. Our future high-resolution transmission electron microscopy studies should be able to elucidate the structural details of the intercalation and deintercalation processes in this unusual host.

ACKNOWLEDGMENTS

We acknowledge the National Science Foundation for support through Grant DMR 91-06792. We also thank the Center for Solid State Science for the use of its Materials Facility in the Goldwater Materials Science Laboratories.

REFERENCES

1. F. Jellinek, *J. Less Common Met.* **4,** 9 (1962).
2. A. Thompson, F. Gamble, and J. Revelli, *Solid State. Commun.* **9,** 981 (1971).
3. P. M. Williams, G. S. Parry, and C. B. Scruby, *Philos. Mag.* **29,** 695 (1974).
4. J. A. Wilson, F. J. Di Salvo, and S. Mahajan, *Phys. Rev. Lett.* **32,** 882 (1974).
5. S. Bayliss, A. Ghorayeb, and D. Guy, *J. Phys. C* **17,** L533 (1984).
6. R. Coleman, W. McNairy, C. Slough, P. Hansma, and B. Drake, *Surf. Sci.* **181,** 112 (1987).
7. R. Coleman, B. Giambattista, P. K. Hansma, A. Johnson, W. McNairy, and C. G. Slough, *Adv. Phys.* **37,** 559 (1988).
8. R. E. Thomson, U. Walter, E. Ganz, J. Clarke, A. Zettl, P. Raunch, and F. J. Di Salvo *Phys. Rev. B* **38,** 10734 (1988).
9. A. M. Ghorayeb and R. H. Friend, *J. Phys. C.* **20,** 4181 (1987); A. M. Ghorayeb, Ph.D. dissertation, Cambridge University, 1985.
10. R. H. Friend and A. D. Yoffe, *Adv. Phys.* **36,** 1 (1987).
11. M. J. McKelvy and W. S. Glaunsinger, *Annu. Rev. Phys. Chem.* **41,** 497 (1990); L. Brown, Ph.D. dissertation, Arizona State University, 1997.
12. J. Rouxel, *in* "Chemical Physics of Intercalation" (A. P. Legrand and S. Flandrois, Eds.), p. 127, Plenum Press, New York, 1982.
13. B. G. Silbernagel and M. S. Whittingham, *J. Chem. Phys.* **64,** 3670 (1976).
14. R. Schöllhorn, H. D. Zagefka, T. Butz, and A. Lerf, *Mater. Res. Bull.* **14,** 369 (1979).
15. F. R. Gamble, J. H. Osiecki, M. Cais, R. Pisharody, F. J. DiSalvo, and T. H. Geballe, *Science* **174,** 493 (1971).
16. L. Bernard, M. J. McKelvy, W. S. Glaunsinger, and P. Colombet, *Solid State Ionics* **15,** 301 (1985).
17. J. Dunn and W. S. Glaunsinger, *Solid State Ionics* **27,** 285 (1988).
18. R. Schöllhorn and H. D. Zagefka, *Angew. Chem. Int.* (*Ed. Engl.*) **16,** 199 (1977).
19. F. R. Gamble and B. G. Silbernagel, *J. Chem. Phys.* **63,** 2544 (1975).
20. C. Riekel, *Solid State Commun.* **28,** 385 (1978).
21. P. F. McMillan, V. Cajipe, P. Molinie, M. F. Quinton, V. Gourlaouen, and P. Colombet, *Chem. Mater.* **3,** 796 (1991).
22. C. Riekel, H. Reznik, R. Schöllhorn, and C. J. Wright, *J. Chem. Phys.* **70,** 5203 (1979).
23. E. Ong, J. Eckert, L. Dotson, and W. S. Glaunsinger, *Chem. Mater.* **6,** 1946 (1994).
24. M. J. McKelvy and W. S. Glaunsinger, *Solid State Ionics* **25,** 287 (1987).
25. J. F. Revelli, *Inorg. Synth.* **19,** 35 (1979).
26. H. J. Bouwmeester, G. A. Wiegers, and C. F. Van Bruggen, *J. Solid State Chem.* **70,** 58 (1987).
27. R. M. A. Lieth and J. C. Terhell, *in* "Preparation and Crystal Growth of Materials with Layered Structures" (R. M. A. Lieth, Ed.), p. 186, Reidel, Dordrect, 1977.
28. G. Hägg and N. Schönberg, *Ark. Kemi* **7,** 371 (1954).
29. Udupa, M. Ramakrishna, and G. Aravamudan, *Current Science* **9,** 206 (1970).
30. S. R. Heller and G. W. A. Milne, "EPA/NIH Mass Spectral Data Base," Vol. 1, p. 1, 1978.
31. M. J. McKelvy and W. S. Glaunsinger, *Solid State Ionics* **34,** 211 (1989).
32. J. Dunn, Ph.D. dissertation, Arizona State University, 1988.
33. M. Dines and R. Levy, *J. Phys. Chem.* **79,** 1979 (1975).
34. M. J. McKelvy and W. S. Glaunsinger, *J. Solid State Chem.* **67,** 142 (1987).
35. M. J. McKelvy, M. Sidorov, A. Marie, R. Sharma, and W. S. Glaunsinger, *Chem. Mater.* **6,** 2233 (1994).
36. F. Jellinek, *Ark. Kemi* **20,** 447 (1962).

37. D. W. Murphy, F. Di Salvo, G. W. Hull Jr., J. V. Waszczak, S. F. Mayer, G. R. Stewart, S. Early, J. V. Acrivos, and T. H. Geballe, *J. Chem. Phys.* **62,** 967 (1975).
38. L. Diebolt, R. Sharma, M. J. McKelvy, and W. S. Glaunsinger, *Mater. Res. Soc. Symp. Proc.* **404,** 183 (1996).
39. C. Riekel, H. G. Reznik, and R. Schöllhorn, *J. Solid State Chem.* **34,** 253 (1980).
40. J. G. Hooley, *Mater. Sci. Eng.* **31,** 17 (1977).
41. J. G. Hooley, *Carbon* **18,** 82 (1980).
42. G. Kirczenow, *in* "Graphite Intercalation Compounds I" (H. Zabel and S. A. Solin, Eds.), p. 59, Springer-Verlag, Berlin, 1990.
43. L. Diebolt, Ph.D. dissertation, Arizona State University, 1996.
44. M. Sidorov, Ph.D. dissertation, Arizona State University, 1995.